2007-01-0735

Analysis of Collisions Involving Articulated Vehicles

R. Matthew Brach
Brach Engineering, LLC

Raymond M. Brach
Brach Engineering, LLC
University of Notre Dame

Copyright © 2007 SAE International

ABSTRACT

In the vast majority of impacts involving light vehicles, traditional impulse-momentum collision models can be used to analyze the mechanics of two colliding vehicles. However, these models cannot handle the multiple degrees of freedom associated with articulated (pin-connected) vehicles. In addition, collisions involving one or two articulated vehicles may not satisfy the basic assumptions of these traditional collisions models. In particular, the assumption that impulses of external forces (such as tire-road friction) are negligible compared to the impulse developed over the crash surface may not be valid. The large masses, long dimensions, the presence of the pinned joint, or all of these factors, may necessitate special considerations and more flexible model capabilities.

This paper lists the assumptions that underlie the application of the principle of impulse and momentum to a planar collision between rigid bodies. The general impact equations involving a pair of pinned rigid bodies are derived and presented. These equations form a set of linear algebraic equations that requires a numerical solution. An example is presented that demonstrates the need to include the capability of modeling the impulses of forces external to the intervehicular contact surface. Results of the model, correlated with data from a controlled experimental collision, follow the presentation of the equations. Another example is then presented that illustrates the application of a velocity constraint to one of the bodies.

INTRODUCTION

A plethora of information is available about the methods that permit the reconstruction of a wide range of collisions involving the impact of single (nonarticulated) vehicles such as cars and light trucks. These methods include those based on Newton’s Laws (planar impact mechanics) and those based on the estimation of the energy associated with residual crush. Accidents involving light vehicles comprise the majority of automotive collisions so these methods provide great utility. Methods based on planar impact mechanics also can be applied to the analysis of collisions involving larger, heavier vehicles, such as straight trucks, as long as the underlying assumptions are reasonably well satisfied. However, analysis of collisions that involve articulated vehicles (a vehicle comprised of two or more distinct interconnected bodies coupled by a pin joint), such as an over-the-road truck tractor and an attached semitrailer or a light vehicle pulling a semitrailer, might not meet the underlying assumptions. Therefore, more sophisticated reconstruction methods may be required to analyze such collisions.

An analysis of the planar motion of a single body requires the use of three coordinates, the two rectilinear coordinates of the mass center and the body’s rotational coordinate. In engineering mechanics, such a body is said to possess three degrees of freedom. Two bodies, each with three degrees of freedom, comprise a single system that has a total of six degrees of freedom. However, if the two bodies are interconnected by a pinned joint, the pin constrains the combined motion. Such a constraint reduces the freedom of the motion in two directions and so the total degrees of freedom of the combined, articulated system of two rigid bodies is reduced from six to four. Hence, four coordinates are necessary and sufficient to fully describe the position and orientation of a single articulated vehicle. In addition, an impact involving one or more articulated vehicles may not satisfy the same assumptions as for two vehicles each comprised of a single mass. In particular, the effect of the frictional forces between some or all of the vehicle tires and the roadway may not be negligible. The effect of additional degrees of freedom and the significance of external impulses must be dealt with explicitly in order to be able to carry out an accurate analysis of an impact involving one or more articulated vehicles.

Before considering the general problem of articulated vehicle impact, it is noted that the planar impact mechanics model [1] may still be used to reconstruct some collisions involving one or more articulated vehicles. Indeed, for an accident where a tractor semitrailer is involved in an impact with a non-articulated vehicle in which the velocities of the centers of mass of the tractor and the semitrailer remain essentially collinear between the onset of impact to separation (such as shown in Figure 1-a) impact mechanics of vehicles that are not articulated, or nonarticulated vehicle impact mechanics, can typically be used to accurately model the impact. Judgement on the part of the collision reconstructionist is required to assess the appropriate applicability of nonarticulated vehicle impact mechanics for accidents involving one or two articulated vehicles.

A model is presented in this paper that can be applied to the impact of a pair of vehicles of which one or both may be articulated. To a certain extent, the development is a generalization of the planar impact mechanics model [1]. Both models are based on the direct application of Newton's Laws through the use of the principle of impulse and momentum. However, the model developed here is more general than the previous development in that it takes into account the constrained degrees of freedom of pin-connected bodies. The model was originally presented by Brach [2] and also provides a more general solution to the problem as the treatment incorporates a moment impulse at the intervehicular contact surface as presented in Brach [3,8]. The more general treatment also introduces additional modeling flexibility by allowing an externally applied impulse and/or velocity constraint to one of the rigid bodies of each of the articulated vehicle pairs. A value of the moment impulse equal to zero, in combination with no pin-connected bodies and no application of external impulses, reduces this model to that presented previously [1].

Accident reconstruction literature concerning the topic of impact between two vehicles including at least one articulated vehicle is scant particularly in comparison to the literature related to the modeling of an impact between two nonarticulated vehicles. To date, there has not been a formulation of the CRASH3 ΔV mechanics involving articulated vehicles. Certain implementations of the software program SMAC (Simulation Model of Automobile Collisions) include the capability of modeling the impact of articulated vehicles. This capability is highlighted in an article by Leonard, et al. [4] which considers the capability of the HVE [5] computer program with comparison of the results of the program to experimental data. Another version of the SMAC algorithm, referred to as *m-smac* [9], has been augmented to include collisions that involve articulated vehicles.

An impact model that includes articulated vehicles, which uses an approach similar to that presented here, was presented by Steffan and Moser [6]. In that paper, the authors consider some of the issues that will be presented later in this paper including the topic of the necessity and use of external impulses.

This paper initially presents the assumptions that underlie the general application of the principle of impulse and momentum to a planar collision between rigid bodies. Prior to the development of the impact equations, an example is presented that demonstrates the need to include the capability of modeling the impulses of forces external to the contact surface. An example, which validates the model using experimental data, follows the presentation of the equations. An example that shows the use of the application of a constraint to one of the vehicles is then presented.

ASSUMPTIONS FOR APPLICATION OF PLANAR IMPACT MECHANICS TO ARTICULATED VEHICLES

The application of planar impact mechanics to vehicle collisions requires that various assumptions about the nature of the collision be satisfied. These assumptions are:

1. only a single impact occurs between only two of the articulated rigid bodies (if multiple impacts occur, each must be analyzed separately),
2. the time duration of intervehicular contact is short (typically on the order of 100 msec to 200 msec); this short time duration implies:
   a. changes in both linear and angular positions of all vehicles during the contact duration are small, and
   b. impulses acting on the vehicles due to external forces (typically tire-pavement frictional forces) are small in comparison to the impulse due to the intervehicular force,

3. the location of the resultant intervehicular impulse is known or can be reasonably estimated,

4. changes in the physical geometry of the masses (such as due to the crush deformation) either are small and can be neglected or are known and can be taken into account, and

5. the effects of any out of (horizontal) plane dynamics are small.

Relatively high speed [>~ 20 mph (32 km/h) closing speed] collisions between light vehicles (cars, sport utility vehicles, pickup trucks, etc.) typically meet all of these assumptions and planar impact mechanics can be applied directly. However, collisions involving one or two articulated vehicles may not meet all of the above assumptions. The large masses, long dimensions or the presence of the pinned joint, or all of these, associated with either of the two masses associated with an articulated vehicle may require special methods associated with assumption 2-b.

As an illustration of this concept, consider a collision in which a tractor semitrailer with no cargo is traveling through an intersection. A large pickup truck, traveling at a high speed, collides with the semitrailer at, and perpendicular to, its rearmost axle. As a result of the impact, the lateral forces of the tires of the semitrailer overcome pavement friction and develop significant lateral slip such that the semitrailer undergoes a rotational velocity change. While the semitrailer undergoes this change in rotational motion, the tractor and its wheels continue to roll in their preimpact direction without any significant change in rotational (yaw) velocity or a change in lateral velocity. Application of the planar impact mechanics model to a collision such as this will fail to accurately predict the velocity changes of the masses. The effect of a large tire-pavement frictional forces such as those that maintain the heading of the tractor in this example can be taken into account using a zero-velocity-change constraint and other special methods introduced in the following sections.

A better understanding of the magnitude of external impulses is illustrated in the following example. The example compares the magnitude of the contact and tire force impulses for an impact between two light vehicles with an impact between a light vehicle and a heavy vehicle. The example illustrates that under certain circumstances assumption 2-b above is not met. The impulse of the tire forces generated by a heavy vehicle can be non-negligible in comparison to the force involved with the intervehicular impulse. Therefore the assumption of negligible external impulses may not always be valid.

EXAMPLE 1 - EXTERNAL IMPULSES

Consider the two collision geometries shown in Figure 1-a and Figure 1-b. Each shows a pair of vehicles at the onset of contact for an inline head-on collision. The first figure shows a tractor semitrailer and a sedan and the second figure shows two sedans. These two collisions are compared under the conditions of no rebound (zero restitution), negligible preimpact and postimpact rotational velocities and a collision duration of about 0.2 seconds. Table 1 lists the relevant vehicular physical data, initial and final velocities and the intervehicular impulses from the analyses. The results in the table are computed using planar impact mechanics.

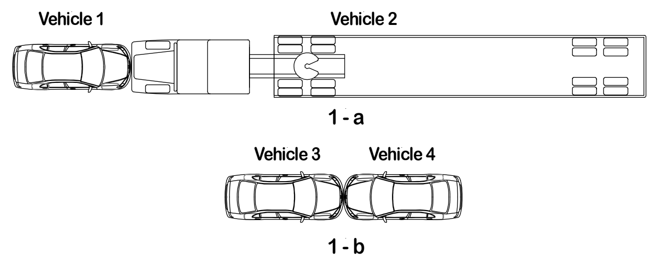

Figure 1-a Inline head-on collision between a tractor semitrailer and a sedan
Figure1-b Inline head-on collision between two sedans

The final speeds and the intervehicular impulses generated for these two collisions were obtained based on the premise that the assumptions for planar impact mechanics were satisfied. In particular, the analyses neglected the impulses generated by any external forces such as tire ground friction. Suppose now that each of vehicles 2 and 4 were in a locked-wheel skid throughout the entire time of contact with tire-to-roadway frictional drag coefficients of $f = 0.6$. The frictional forces generated by skidding tires of vehicles 2 and 4 are F_2 = 158.9 kN (35,718 lb) and F_4 = 14.1 kN (3175 lb), respectively. Assuming that these forces are constant during the 0.2 seconds of contact, their impulses are 31.8 kN-s (7144 lb-s) and 2.8 kN-s (635 lb-s), respectively. Note that the impulse due to the frictional force for vehicle 2 in collision 1-a, 31.8 kN-s (7144 lb-s), is about 63% of the intervehicular contact impulse, 50.6 kN-s (11,367.5 lb-s). Further note that the impulse due to the frictional force for vehicle 4 in collision 1-b, 2.8 kN-s (635 lb-s), is only about 9% of the impulse due to the intervehicular force. ☐

The example above illustrates that impulses from forces external to the contact surface may not be negligible when analyzing a collision that involves a heavy vehicle. Other circumstances can arise where the impulse due to a force other than the intervehicular force may be significant. Consider a 90° front-to-side collision between two vehicles with one of the vehicles pulling a semitrailer. (This collision geometry is considered in a later example. See Figure 4.) Suppose further that the wheels of the semitrailer are freely rolling prior to impact and remain in that condition from the onset of contact to separation. This implies that the lateral forces generated by the wheels on the semitrailer do not exceed the frictional limit and the semitrailer axle does not develop a lateral velocity change. If the longitudinal velocity of the tow vehicle and the semitrailer are small, this situation acts, in effect, as though the semitrailer is constrained in the lateral direction by tire friction. This and Example 1 illustrate that a need exists for the articulated vehicle impact model to handle velocity constraints as well as external impulses.

ARTICULATED VEHICLE IMPACT EQUATIONS

In this section a generalized 4-body impact model is presented. Figure 2 shows the free body diagrams of the four masses that comprise two articulated vehicles, entitled Vehicle A and Vehicle B. Vehicle A consists of Bodies 1 and 3 (shown shaded in the figure) and Vehicle B consists of bodies 2 and 4. (A larger version of Figure 2 is included at the end of the paper for clarity.) In addition to the various impulses required for the analysis, the figure also shows the variables and the coordinate systems associated with the model development. The x-y coordinate system is fixed to the ground and the n-t coordinate system is at an angle Γ relative to the x-y system.

Dynamic contact is between Body 1 and Body 2 and creates an impulse P with components P_x and P_y and a moment impulse, M. Bodies 1 and 3 are interconnected by a frictionless pin that transmits an impulse R with components R_x and R_y. Bodies 2 and 4 are interconnected by a frictionless pin that transmits an impulse Q with components Q_x and Q_y. Allowance is made for an external impulse C_3, applied to Body 3 and an external impulse C_4, applied to Body 4. Impulses C_3 and C_4 are shown in the figure using their x and y components. Impulses C_3 and C_4 are arbitrary (they can be zero) and are developed by placing final velocity constraints at respective locations on Bodies 3 and 4.

The model requires that the contact take place between Bodies 1 and 2 only. However, this requirement does not imply that either Body 1 and 2 necessarily represent a tow vehicle. In this way the model can accommodate the impact between the two tractors, the two semitrailers, or between the tractor of one tractor semitrailer combination and the semitrailer of the other combination.

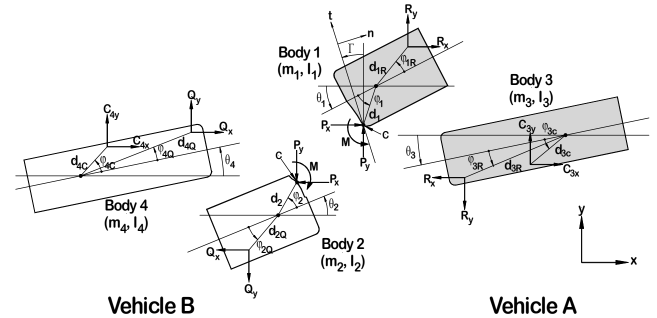

Figure 2 Free Body Diagrams for the four masses in a collision between two articulated vehicles

In Figure 2 the variables P, Q, R, C_3 and C_4 represent the *impulses* of the forces that act at those locations, not the forces themselves. Similarly, M represents the *moment impulse* that can act at the contact surface. The inclusion of the moment impulse at the contact surface permits the modeling of, for example, the structural engagement over the intervehicular contact surface that can transmit angular momentum from one vehicle to the other. While experience indicates that a non-zero contact moment is not necessarily a common occurrence during vehicular collisions, the inclusion of the moment impulse in the model provides for greater generality.

As will be shown later, a moment coefficient, e', is needed in the formulation of the problem to relate the final angular velocities of the vehicles [3, 8]. The impulse P represents the intervehicular impulse that acts at a point on the contact surface, C, called the *impact center*. This point represents the spatial and temporal average of the location of the application of the impulse P during contact between the two bodies. Determination of the location of the impulse center requires judgement by the user in applications of this model.

The orientations of the bodies relative to the ground at the time of impact are indicated by the heading angles θ_1, θ_2, θ_3, and θ_4, all defined relative to the x-y coordinate axes. All impulses are located relative to the mass center of each body and heading orientation by a distance, d, and an angle φ. For example, the impulse P and the impact center are located relative to the centers of mass of Bodies 1 and 3 by distances d_1 and d_3, respectively, acting at angles φ_1 and

φ_3, respectively. The location of the hitch pin is defined on Body 1 by d_{1R} and φ_{1R} and on Body 3 by d_{3R} and φ_{3R}. The hitch pin location is defined on Body 2 with d_{2Q} and φ_{2Q} and on Body 4 with d_{4Q} and φ_{4Q}. The external impulses C_3 and C_4 act on Bodies 3 and 4 at distances d_{3C} and d_{4C} from the center of mass, at angles φ_{3C} and φ_{4C}, respectively. A normal and tangential coordinate system, (n, t), is referenced to the crush surface and is oriented with respect to the x-y coordinate system by the angle Γ. Bodies 1 through 4 have mass m_1, m_2, m_3, and m_4, and rotational yaw inertias I_1, I_2, I_3, and I_4, respectively.

Before proceeding with the development of the equations that govern the impact between two articulated vehicles, some additional discussion of the impulses shown on the free body diagrams is required. The impulses C_3 and C_4 are included in the free body diagrams of Bodies 3 and 4, respectively, and are intended to be externally applied impulses, remote from the intervehicular contact impulse, P. The impulses Q and R are the impulses generated at the hitch pins that maintain a translational velocity constraint at each pin. The constraint is imposed such that the final velocity components of the two pinned bodies at each hitch point are identical.

Therefore, the components of these impulses, R_x and R_y for Bodies 1 and 3 and Q_x and Q_y for Bodies 2 and 4, are shown in the figure acting equal and opposite on each pair of bodies. The components of the intervehicular impulse, P_x and P_y, are shown on Bodies 1 and 3. The lines of action of these impulse components are the same on each body but the direction of the action of each is opposite, consistent with Newton's Third Law. Similarly, the moment impulse M acting along the contact surface is also shown acting on both Bodies 1 and 2 with opposite directions.

The development that follows is a direct application of the principle of impulse and momentum [7] to each body of the system of pairs of (pinned) rigid bodies. This principle states that the change in (linear and angular) momentum of a rigid body is equal to the sum of the external (linear and angular) impulses acting on that body. The application of the principle initially produces twelve scalar equations, three for each of the four masses.

As will be seen, the development of the equations involves more than twelve unknowns and additional equations are needed to solve the problem. Consistent with the notation used in the formulation of the planar impact mechanics solution, the variables associated with the preimpact velocities are shown in lower case, such as v_{3x}, and the variables associated with the postimpact velocities are shown in upper case, such as V_{2y}. All of the variables used in these equations are listed in a table in Appendix A. The equations are also repeated in Appendix A for convenience. The impulse and momentum equations are as follows:

For Body 1:

$$m_1(V_{1x} - v_{1x}) = P_x + R_x \tag{1}$$

$$m_1(V_{1y} - v_{1y}) = P_y + R_y \tag{2}$$

$$\begin{aligned} I_1(\Omega_1 - \omega_1) = M &+ d_1 \sin(\theta_1 + \varphi_1)P_x - \\ &d_1 \cos(\theta_1 + \varphi_1)P_y - \\ &d_{1R} \sin(\theta_1 + \varphi_{1R})R_x + \\ &d_{1R} \cos(\theta_1 + \varphi_{1R})R_y \end{aligned} \tag{3}$$

For Body 2:

$$m_2(V_{2x} - v_{2x}) = -P_x - Q_x \tag{4}$$

$$m_2(V_{2y} - v_{2y}) = -P_y - Q_y \tag{5}$$

$$\begin{aligned} I_2(\Omega_2 - \omega_2) = -M &+ d_2 \sin(\theta_2 + \varphi_2)P_x - \\ &d_2 \cos(\theta_2 + \varphi_2)P_y - \\ &d_{2Q} \sin(\theta_2 + \varphi_{2Q})Q_x + \\ &d_{2Q} \cos(\theta_2 + \varphi_{2Q})Q_y \end{aligned} \tag{6}$$

For Body 3:

$$m_3(V_{3x} - v_{3x}) = -R_x + C_3 \cos\alpha_3 \tag{7}$$

$$m_3(V_{3y} - v_{3y}) = -R_y + C_3 \sin\alpha_3 \tag{8}$$

$$\begin{aligned} I_3(\Omega_3 - \omega_3) = &-d_{3R} \sin(\theta_3 + \varphi_{3R})R_x + \\ &d_{3R} \cos(\theta_3 + \varphi_{3R})R_y + \\ &d_{3C} \sin(\theta_3 + \varphi_{3C})C_3 \cos\alpha_3 - \\ &d_{3C} \cos(\theta_3 + \varphi_{3C})C_3 \sin\alpha_3 \end{aligned} \tag{9}$$

For Body 4:

$$m_4(V_{4x} - v_{4x}) = -Q_x + C_4 \cos\alpha_4 \tag{10}$$

$$m_4(V_{4y} - v_{4y}) = Q_y + C_4 \sin\alpha_4 \tag{11}$$

$$\begin{aligned} I_4(\Omega_4 - \omega_4) = &-d_{4Q}\sin(\theta_4 + \varphi_{4Q})Q_x + \\ &d_{4Q}\cos(\theta_4 + \varphi_{4Q})Q_y - \\ &d_{4C}\sin(\theta_4 + \varphi_{4C})C_4\cos\alpha_4 + \\ &d_{4C}\cos(\theta_4 + \varphi_{4C})C_4\sin\alpha_4 \end{aligned} \tag{12}$$

Counting equations and unknowns gives twelve equations, 1 through 12, and twenty-one unknowns: V_{1x}, V_{1y}, V_{2x}, V_{2y}, V_{3x}, V_{3y}, V_{4x}, V_{4y}, Ω_1, Ω_2, Ω_3, Ω_4, M, P_x, P_y, R_x, R_y, Q_x, Q_y, C_3, and C_4. For the general problem that involves all of the unknowns, nine more equations are needed to make the problem tractable. Note that while the general problem involves the twenty-one unknowns listed above, most problems will likely involve only a subset of these. For example, if one of the vehicles is not articulated, three of the unknown velocities and the associated hitch impulses do not appear in the formulation.

The remaining nine equations required in the general formulation are introduced from four sources:

1) the consideration of the normal and tangential contact processes over the intervehicular contact surface,
2) the existence of a moment impulse over the intervehicular contact surface,
3) the constraints imposed on the system at the hitch, and
4) the velocity constraints, if any, imposed on Bodies 3 and 4.

Impulses R_x, R_y, Q_x, Q_y, C_3, and C_4 are related to the velocity constraints, and are determined through the imposition of constraint equations.

A thirteenth equation is obtained from the impulse ratio coefficient, μ, defined previously [1] as the ratio of the tangential to normal impulse components. This is:

$$P_t = \mu P_n \tag{13a}$$

or, using the *x-y* components of the impulses,

$$P_y\cos\Gamma - P_x\sin\Gamma = \mu(P_y\sin\Gamma + P_x\cos\Gamma) \tag{13b}$$

Another equation is obtained from the definition of the coefficient of restitution, *e*, in the normal direction, *n* (as defined by Γ), at the impact center. The coefficient of restitution is defined as the ratio of the relative normal velocity **at the impact center** (shown as point C in Figure 2) at the end of contact to the relative normal velocity at the impact center at the beginning of contact:

$$e = -\frac{V_{Crn}}{v_{Crn}} \tag{14}$$

where

$$\begin{aligned} V_{Crn} = &-[V_{1x} + d_1\sin(\theta_1 + \varphi_1)\Omega_1]\cos\Gamma + \\ &[V_{1y} - d_1\cos(\theta_1 + \varphi_1)\Omega_1]\sin\Gamma - \\ &[V_{2x} - d_2\sin(\theta_2 + \varphi_2)\Omega_2]\cos\Gamma - \\ &[V_{2y} + d_2\cos(\theta_2 + \varphi_2)\Omega_2]\sin\Gamma \end{aligned} \tag{15}$$

$$\begin{aligned} v_{Crn} = &[v_{1x} + d_1\sin(\theta_1 + \varphi_1)\omega_1]\cos\Gamma + \\ &[v_{1y} - d_1\cos(\theta_1 + \varphi_1)\omega_1]\sin\Gamma - \\ &[v_{2x} - d_2\sin(\theta_2 + \varphi_2)\omega_2]\cos\Gamma - \\ &[v_{2y} + d_2\cos(\theta_2 + \varphi_2)\omega_2]\sin\Gamma \end{aligned} \tag{16}$$

The moment restitution at the surface [3,8] leads to the following equation:

$$e'M = -(1+e')(\Omega_2 - \Omega_1)\bar{I} \tag{17a}$$

where

$$\bar{I} = \frac{I_1 I_2}{I_1 + I_2} \tag{17b}$$

Note that for $e' = 0$, the vehicles will have the same postimpact angular velocity, that is, $\Omega_1 = \Omega_2$. This condition corresponds to a perfectly inelastic angular impact, and is independent of the coefficient of restitution, *e*, defined in Eq. 14. For $e' = -1$, the moment impulse M is zero and corresponds to a rigid body collision in which the moment impulse can be neglected.

Two constraints are imposed on the system that require that the hitch point for each of the two pairs of bodies have the same final linear velocity components. It is assumed that no impulsive moments act at the hitch location. The velocity constraint imposed on one pair of masses yields two equations, one for each velocity component along the *x-y* coordinate system. This gives a total of four more equations, two each for each vehicle. The hitch constraint is imposed on the postimpact velocities. (Note that to be physically realistic, compatible initial velocities must be used that satisfy the pin constraints.)

For Vehicle A at the hitch point, *R*, in the *x*-direction:

$$V_{1x} - d_{1R}\sin(\theta_1 + \varphi_{1R})\Omega_1 = V_{3x} + d_{3R}\sin(\theta_3 + \varphi_{3R})\Omega_3 \quad (18)$$

For Vehicle A at the hitch point, *R*, in the *y*-direction:

$$V_{1y} + d_{1R}\cos(\theta_1 + \varphi_{1R})\Omega_1 = V_{3y} - d_{3R}\cos(\theta_3 + \varphi_{3R})\Omega_3 \quad (19)$$

For Vehicle B at the hitch point, *Q*, in the *x*-direction:

$$V_{2x} + d_{2Q}\sin(\theta_2 + \varphi_{2Q})\Omega_2 = V_{4x} - d_{4Q}\sin(\theta_4 + \varphi_{4Q})\Omega_4 \quad (20)$$

For Vehicle B at the hitch point, *Q*, in the *y*-direction:

$$V_{2y} - d_{2Q}\cos(\theta_2 + \varphi_{2Q})\Omega_2 = V_{4y} + d_{4Q}\cos(\theta_4 + \varphi_{4Q})\Omega_4 \quad (21)$$

As described previously, circumstances in a collision involving an articulated vehicle may require that the final velocity of one of the bodies be constrained to a certain direction due to interactions with other environmental objects (such as a curb, friction, etc.). The development of the impact model therefore includes additional impulses, C_3 and C_4, to facilitate the inclusion of constraints on the velocities of Bodies 3 and 4. Of course, these constraints may not exist or may not be applied to all problems.

Note that one restriction of the development of the model is that the location of a velocity constraint and the impact center cannot be the same. For example, consider the impact between the tractor of one tractor semitrailer combination into the semitrailer of another tractor semitrailer combination. In this case, Body 1 of Vehicle A is the tractor involved in the impact, with Body 3 assigned to the semitrailer. Body 2 (the other body involved in the impact) will be assigned as the semitrailer of Vehicle B, with Body 4 as the tractor of Vehicle B. Since the impact is between Body 1 and Body 2, a velocity constraint can be applied to the semitrailer of Vehicle A (Body 3) or the tractor of Vehicle B (Body 4).

While the model can be applied to two single vehicles ($m_3 = m_4 = 0$ and $I_3 = I_4 = 0$) the development dictates that the model cannot accommodate velocity constraints applied to these two single vehicles. If the circumstances of the collision require such a need, the hitch impulses *R* and *Q* are permitted to be specified and can be used for the purpose of achieving a velocity constraint depending on the implementation of the solution.

Figure 3 shows the geometric configuration of constraint velocity, Figure 3(a), and the constraint impulse, Figure 3(b). The variables in the figure are given a general subscript, *i*, which can take on the value 3 or 4 depending on the body to which the constraint applies. The angle α_i is defined in the *x-y* coordinate system as shown. The velocity constraint, from Figure 3(a), takes the form:

$$V_{ix}\cos\alpha_i + V_{iy}\sin\alpha_i = 0,\ i = 3,4 \quad (22)$$

The direction of the constraint impulse at the location where the velocity constraint is imposed acts perpendicular to the direction defined by α_i as shown in Figure 3(b). Expanding this expression for each of the Bodies 3 and 4 with the appropriate kinematics gives:

$$[V_{3x} + d_{3C}\sin(\theta_3 + \varphi_{3C})\Omega_3]\cos\alpha_3 + [V_{3y} - d_{3C}\cos(\theta_3 + \varphi_{3C})\Omega_3]\sin\alpha_3 = 0 \quad (23)$$

$$[V_{4x} - d_{4C}\sin(\theta_4 + \varphi_{4C})\Omega_4]\cos\alpha_4 + [V_{4y} + d_{4C}\cos(\theta_4 + \varphi_{4C})\Omega_4]\sin\alpha_4 = 0 \quad (24)$$

Figure 3(b) shows the direction of the components of the impulse that act to restrict the velocity to the direction specified by α_i.

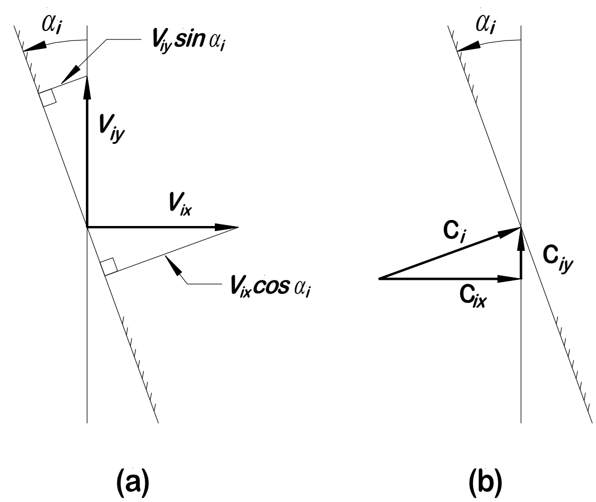

Figure 3 Geometry of the velocity constraints

In addition to the original twelve equations from impulse momentum, an inventory of the equations now gives the additional nine equations, 13, 14, 17, 18, 19, 20, 21, 23, and 24 bringing the total number of equations to twenty-one. For the full complement of masses and conditions, the number of equations equals the number of unknowns and the problem can be solved. Additional complexities exist due to the various configurations of vehicles and combination of conditions that may be required in the reconstruction of a collision. For example, if there are no velocity constraints ($C_3 = C_4 = 0$), then the total number of equations and unknowns is reduced by two and becomes nineteen.

The equations are algebraic and linear and the solution can be implemented in a computer program. Such an implementation permits the analysis of collisions of various geometries involving combinations of articulated and nonarticulated vehicles. Several examples are now presented to demonstrate the utility of the model.

Equations 1 through 24 (with the exception of Eqs 15, 16 and 22) provide a system of linear algebraic equations with the twenty-one unknown final velocity components and impulse components listed above. If the initial velocities, impact coefficients, vehicle physical properties, body configurations and constraint velocities are known, the equations can be used to solve for the unknown final velocity components and impulses for a given set of initial velocities. If only one final velocity constraint exists, the number of equations and unknowns is reduced by one; with no constraints, the number reduces to nineteen. Under any circumstances, a numerical solution is necessary. As presented previously [1], a critical value of the impulse ratio $\mu = \mu_0$ corresponds to the condition that the relative tangential velocity between the bodies in contact ceases prior to separation.

VALIDATION OF THE ARTICULATED VEHICLE IMPACT EQUATIONS USING EXPERIMENTAL DATA

It is instructional to examine the equations presented above relative to experimental data. Data used for model validation by Steffan and Moser [6] is also used here [10]. In the staged collision, an Alfa Romeo 164 sedan pulling a Hobby - 495 travel trailer is impacted on the right front door by the front of an Opel Ascona C 4-door sedan. Figure 4 shows the relative locations and orientations of the vehicles at the onset of contact. Table 2 lists some of the physical parameters of the test vehicles and also some of the test values. Figure 5 shows the two vehicles at the onset of contact and depicts several of the model parameters that are needed for the analysis.

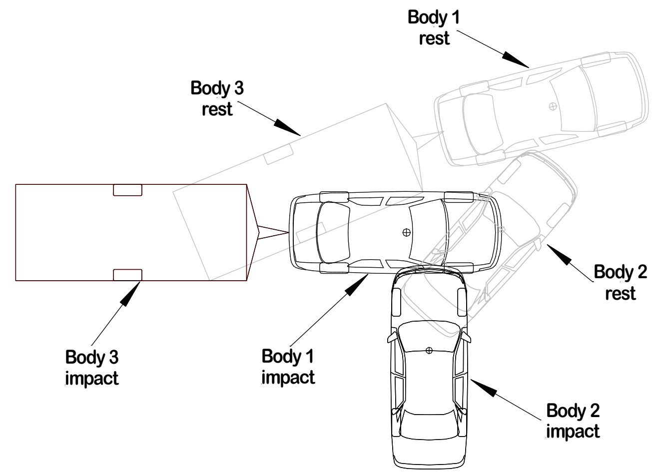

Figure 4 Diagram of the relative positions and orientations of the test vehicles at the onset of impact and at rest

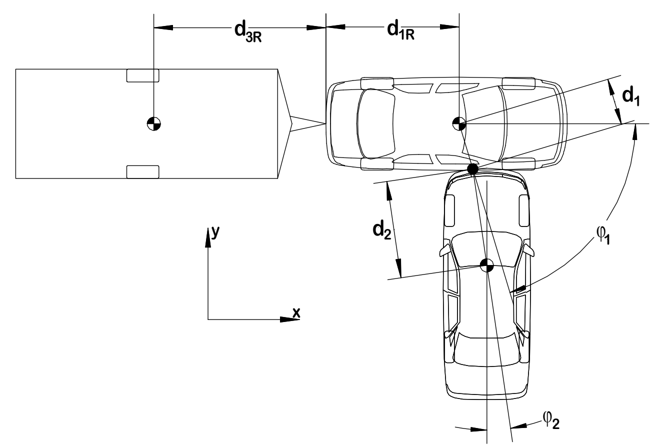

Figure 5 Diagram that shows the vehicles at the onset of contact, the location of the impact center and several of the model parameters needed for the analysis

The postimpact speeds from the test were available for the Alfa Romeo and the Ascona only [10]. No data was reported for the travel trailer. Therefore the comparison between the test speeds and the speeds predicted by the analysis using the articulated vehicle impact model will be done for Bodies 1 and 2 only. Comparison will be made between the preimpact and postimpact kinetic energy of the system. The graphs in Figures 6a and 6b show the magnitude of the velocity components of the center of mass v_x, v_y, v, and the rotational velocity of the vehicles determined from the test data as a function of time for the Alfa Romeo and the Ascona, respectively. The data indicate that the impulse duration was approximately 0.15 seconds. The change of the velocity of the center of mass of the Alfa Romeo, ΔV, is about 22.5 kph (14.0 mph) with individual values of the velocity changes of $\Delta v_x = 6.5$ kph (4.0 mph) and $\Delta v_y = 21.5$ kph (13.4 mph). The change of the velocity of the center of mass of the Opel Ascona, ΔV, is about 34.3 kph (21.3 mph) with individual values of the velocity changes of $\Delta v_x = 7.5$ kph (4.7 mph) and $\Delta v_y = 33.5$ kph (20.8 mph).

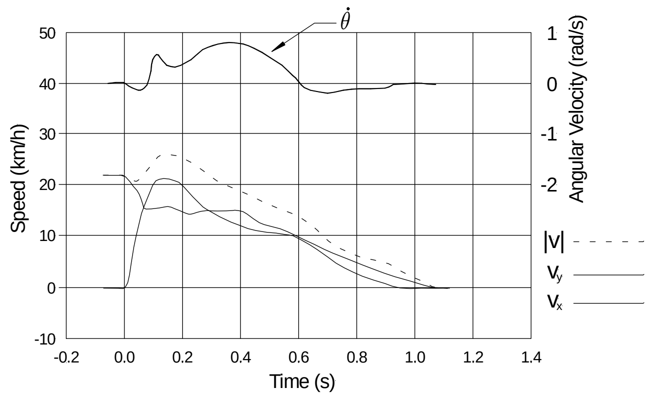

Figure 6a Data showing the velocity of the mass center of the Alfa Romeo and its angular velocity as a function of time with contact initiated at time = 0 seconds

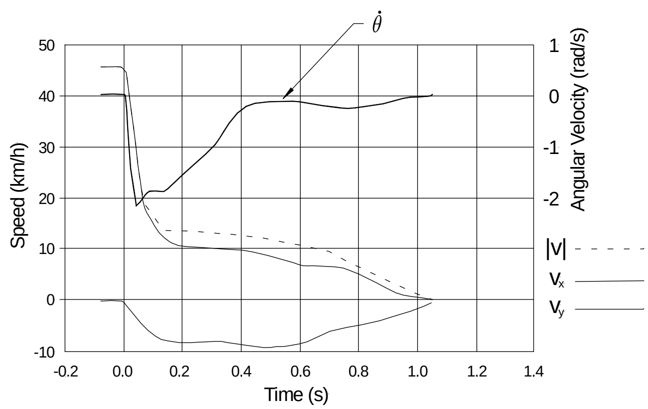

Figure 6b Data showing the velocity of the mass center of the Ascona and its angular velocity as a function of time with contact initiated at time = 0 seconds. (Note that due to instrumentation convention the velocity in the *x*-direction is shown as negative in the data, but is positive with respect to the coordinate system shown in Figure 5.)

Sufficient information from the experimental data is present to determine the coefficient of restitution for the collision. Using the *y*-direction as shown in Figure 5 as the positive normal direction, the value of *e* can be determined from the following equation:

$$-e = \frac{V_{Crn}}{v_{Crn}} = \frac{V_{1n} + d_c\Omega_1 - V_{2n} + d_a\Omega_2}{v_{1n} + d_c\omega_1 - v_{2n} + d_a\omega_2} \tag{25}$$

For values of V_{1n} = 21.5 kph (13.4 mph), V_{2n} = 11.5 kph (7.1 mph), v_{1n} = 0.0 kph, v_{2n} = 45.0 kph (28.0 mph), Ω_1 = 0.55 rad/s, Ω_2 = -2.2 rad/s, ω_1 = 0.0 rad/s, and ω_2 = 0.0 rad/s, the coefficient of restitution for the collision is determined to be approximately e = 0.2. Therefore, the analysis performed to compare the model with the test data was conducted using e = 0.2 and $\mu = \mu_0$. For this collision the moment impulse coefficient is set equal to negative one, e' = -1, which makes the moment at the contact surface zero, M = 0. Table 3 shows the comparison of the experimental data with the results of the analysis. Figure 7 (at the end of the paper) depicts the spreadsheet used for the analysis. The numerical results in the figure are for the analysis with e = 0.2 and $\mu = \mu_0$. No velocity constraint was used in this analysis.

The data in Table 3 show good agreement between the experimental results and the analysis. The ΔV of the center of mass of the Alfa Romeo was 22.5 kph (14.0 mph) experimentally with the analysis yielding a value of 23.2 kph (14.4 mph), an error of 3.1%. The ΔV of the center of mass of the Opel Ascona was 34.3 kph (21.3 mph) experimentally with the analysis yielding a value of 34.1 kph (21.2 mph), an error of 0.6%. According to the experimental data, the system lost 46.4% of its initial energy. The analysis predicts a 43.2% energy loss.

A comparison could not be made between the experimental and analytical results for the semitrailer as no experimental results were reported. The good agreement between the analytical results with the experimental data for the Alfa Romeo and the Opel Ascona without the use of a velocity constraint on the semitrailer indicates that a velocity constraint is not needed. However, an analysis of the collision that included a velocity constraint perpendicular to the longitudinal axis of the semitrailer applied at the center of mass using the initial conditions reported in the experimental data was done. The results of that analysis show that the ΔVs of the Opel and the Alfa Romeo change little in magnitude and direction but the angular velocities of the vehicles differ significantly from the experimental data. In particular, the angular velocity of the Alfa Romeo increases by about 130%.

No significant refinement of the analysis was performed to obtain the numbers that were used for comparison. An improvement in the match between the analysis and the experimental data might be obtained with small changes in the location of the impact center. □

Another example is provided that illustrates the use of the capability to impose a velocity constraint during the impact analysis.

EXAMPLE 2 - VELOCITY CONSTRAINT

This example presents the analysis of the speed changes associated with an impact between a tractor semitrailer and a full-size pickup truck where the velocity constraint is used. Consider the impact geometry depicted in Figure 8. The figure shows a pickup truck and a tractor semitrailer at the onset of contact between the front of the pickup truck and the right front wheel of the tractor. Table 4 lists the relevant vehicular physical data, initial and final velocities and the impulse required to impose the velocity constraint determined in the analysis. The impact is modeled for $e = 0.2$ and for $\mu = \mu_0$.

Note that the tractor semitrailer is located immediately adjacent to a utility pole as shown in Figure 8. It is assumed that the utility pole is rigid and does not fail during the impact and therefore acts to restrict the postimpact velocity of the contact point between the semitrailer and the pole to have a zero final velocity in the y-direction. Therefore, a velocity constraint will be imposed on this point of the semitrailer as part of the impact analysis. Note that the location of the utility pole, and therefore the point of application of the constraint, was selected here as collinear with the y-axis and the center of mass of the semitrailer. This is for simplicity and to facilitate the interpretation of the results.

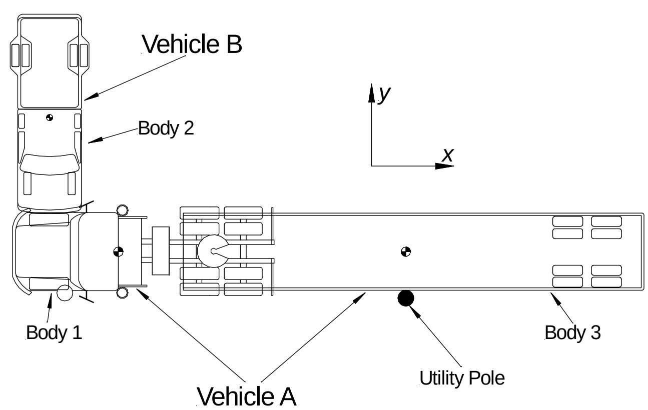

Figure 8 Relative location and orientation of the vehicles at the onset of contact for Example 2

The analysis leads to final velocity of the center of mass of the semitrailer in the y-direction, V_{3y}, is zero. This is consistent with the velocity constraint imposed on the semitrailer located at a point along the y-axis collinear with the center of mass of the semitrailer. For this geometry both the point of application of the constraint and the center of mass of the semitrailer will have the same postimpact velocity in the y-direction. The results of the analysis also provide the magnitude of the impulse applied by the utility pole to the side of the semitrailer to impose the velocity constraint. In this case the impulse is 5874 N-s (1320.5 lb-s). ☐

CONCLUSIONS

It has been shown that collisions involving one or more articulated vehicles, as well as some collisions involving non-articulated vehicles that fail to meet the underlying assumptions of the planar impact mechanics model, require additional modeling flexibility to accurately reconstruct vehicle speeds. This paper demonstrates that the planar impact mechanics model can be extended to provide a more general solution to the impact problem including the capability to introduce external impulses and/or velocity constraints to analyze these collisions.

Note that different combinations of the number of bodies and different combinations of choices of known and unknown impulses and final velocity constraints create a flexibility in the model that can be exploited to cover a wide variety of different reconstruction applications. The model presented here reduces to the single body planar impact mechanics model when the semitrailers are eliminated, no external impulses are applied and no moment is present at the contact surface.

ACKNOWLEDGEMENTS

The authors would like to thank Jim Sprague of Packer Engineering for reading the manuscript and making many useful suggestions for improvement. The authors are also indebted to Bill Cliff of MEA Forensic Engineers for providing the experimental data used in the paper.

REFERENCES

1. Brach, Raymond M. and R. Matthew Brach, *Vehicle Accident Analysis and Reconstruction Methods*, SAE, Warrendale, PA 15096, 2005.

2. Brach, Raymond M., “Impact of Articulated Vehicles,” Paper 860015, SAE International, Warrendale, PA 15096, 1986.

3. Brach, Raymond M., “An Impact Moment Coefficient for Vehicle Collision Analysis,” Paper 770014, *Transactions*, SAE, Warrendale, PA, 1977.

4. Leonard, M., et al., "HVE EDSMAC4 Trailer Model Simulation Comparison with Crash Test Data," Paper 2000-01-0468, SAE International, Warrendale, PA, 15096, 2000.

5. Day, T. D. "An Overview of the EDSMAC4 Collision Simulation Model," Paper 1999-01-0102, SAE International, Warrendale, PA 15096, 1999.

6. Steffan, Hermann and Andreas Moser, "The Trailer Simulation Model of PC-Crash," Paper 980372, SAE International, Warrendale, PA 15096, 1998.

7. Beer, F. P. and E. R. Johnson, *Vector Mechanics for Engineers*, McGraw-Hill Book Company, New York, NY, 1962.

8. Brach, R. M., "Formulation of Rigid Body Impact Problems using Generalized Coefficients," *Int J of Engrg Sci*, Vol 36, 1, p 61-72, 1998.

9. McHenry, B. G. and R. R. McHenry, "SMAC-87," Paper 880227, SAE International, Warrendale, PA 15096, 1987.

10. Test performed in Wildhaus (Switzerland) by DEKRA (Germany) and Winterthur Insurance (Switzerland), 1995.

CONTACT

R. Matthew Brach
Brach Engineering, LLC
50515 Mercury Drive
Granger, IN 46530-8501
matt_brach@brachengineering.com

APPENDIX A - THE IMPACT EQUATIONS

The twenty-one equations formulated for the impact for articulated vehicles presented in this paper can be solved for the twenty-one unknowns of the problem: V_{1x}, V_{1y}, V_{2x}, V_{2y}, V_{3x}, V_{3y}, V_{4x}, V_{4y}, Ω_1, Ω_2, Ω_3, Ω_4, M, P_x, P_y, R_x, R_y, Q_x, Q_y, C_3, and C_4. Prior to implementing a solution, the equations are put into matrix form to facilitate a solution through numerical means. The model can be applied to a wide variety of collision geometries ranging from the impact of two nonarticulated vehicles to two articulated vehicles. Each of the configurations may include velocity constraints and/or externally applied impulses. Each distinct vehicular configuration and combination of conditions leads to a different set of unknowns and a different set of equations to be solved for those unknowns.

Before presenting the equations, the variables that appear in the equations and the notation used in their development are listed.

Notation, Subscripts:

n, t	normal & tangential axes (Fig 2)
x, y	ground based axes (Fig 2)
1, 2	body number
3, 4	body number
C	impact center, velocity constraint
Q	external impulse Q
r	relative
R	external impulse R

Notation, Variables:

C	impulse (velocity constraint)
d_1, d_2	distances (Fig 2)
d_3, d_4	distances(Fig 2)
e	coefficient of restitution
e'	moment coefficient
I	yaw moment of inertia
m	mass of body
M	moment impulse at impact center
P	impulse at impact center
Q	impulse at hitch for Bodies 2 and 4
R	impulse at hitch for Bodies 1 and 3
v	initial velocity
V	final velocity
ΔV	velocity change
α	constraint angle
Γ	crush surface angle
μ	impulse ratio
ω	initial angular velocity
Ω	final angular velocity
φ	angle orientation of impulse of velocity constraint
θ	angular orientation of body

First, the twenty-one equations are repeated here. The equation numbers are sequential for convenience.

$$m_1(V_{1x} - v_{1x}) = P_x + R_x \quad \text{(A1)}$$

$$m_1(V_{1y} - v_{1y}) = P_y + R_y \quad \text{(A2)}$$

$$I_1(\Omega_1-\omega_1)=M+d_1\sin(\theta_1+\varphi_1)P_x-\\ d_2\cos(\theta_1+\varphi_1)P_y-\\ d_{1R}\sin(\theta_1+\varphi_{1R})R_x+\\ d_{1R}\cos(\theta_1+\varphi_{1R})R_y \tag{A3}$$

$$I_2(\Omega_2-\omega_2)=-M+d_2\sin(\theta_2+\varphi_2)P_x-\\ d_2\cos(\theta_2+\varphi_2)P_y-\\ d_{2Q}\sin(\theta_2+\varphi_{2Q})Q_x+\\ d_{2Q}\cos(\theta_2+\varphi_{2Q})Q_y \tag{A4}$$

$$m_2(V_{2x}-v_{2x})=-P_x-R_x \tag{A5}$$

$$m_2(V_{2y}-v_{2y})=-P_y-R_y \tag{A6}$$

$$m_3(V_{3x}-v_{3x})=-R_x+C_3\cos\alpha_3 \tag{A7}$$

$$m_3(V_{3y}-v_{3y})=-R_y+C_3\sin\alpha_3 \tag{A8}$$

$$I_3(\Omega_3-\omega_3)=-d_{3R}\sin(\theta_3+\varphi_{3R})R_x+\\ d_{3R}\cos(\theta_3+\varphi_{3R})R_y\\ +d_{3C}\sin(\theta_3+\varphi_{3C})C_3\cos\alpha_3-\\ d_{3C}\cos(\theta_3+\varphi_{3C})C_3\sin\alpha_3 \tag{A9}$$

$$m_3(V_{3x}-v_{3x})=-R_x+C_3\cos\alpha_3 \tag{A10}$$

$$m_4(V_{4y}-v_{4y})=Q_y+C_4\sin\alpha_4 \tag{A11}$$

$$I_4(\Omega_4-\omega_4)=-d_{4Q}\sin(\theta_4+\varphi_{4Q})Q_x+\\ d_{4Q}\cos(\theta_4+\varphi_{4Q})Q_y-\\ d_{4C}\sin(\theta_4+\varphi_{4C})C_4\cos\alpha_4+\\ d_{4C}\cos(\theta_4+\varphi_{4C})C_4\sin\alpha_4 \tag{A12}$$

$$P_y\cos\Gamma-P_x\sin\Gamma=\mu(P_y\sin\Gamma+P_x\cos\Gamma) \tag{A13}$$

$$e=-\frac{V_{Crn}}{v_{Crn}} \tag{A14}$$

where

$$V_{Crn}=-[V_{1x}+d_1\sin(\theta_1+\varphi_1)\Omega_1]\cos\Gamma+\\ [V_{1y}-d_1\cos(\theta_1+\varphi_1)\Omega_1]\sin\Gamma-\\ [V_{2x}-d_2\sin(\theta_2+\varphi_2)\Omega_2]\cos\Gamma-\\ [V_{2y}+d_2\cos(\theta_2+\varphi_2)\Omega_2]\sin\Gamma$$

$$v_{Crn}=[v_{1x}+d_1\sin(\theta_1+\varphi_1)\omega_1]\cos\Gamma+\\ [v_{1y}-d_1\cos(\theta_1+\varphi_1)\omega_1]\sin\Gamma-\\ [v_{2x}-d_2\sin(\theta_2+\varphi_2)\omega_2]\cos\Gamma-\\ [v_{2y}+d_2\cos(\theta_2+\varphi_2)\omega_2]\sin\Gamma$$

$$e'M=-(1+e')(\Omega_2-\Omega_1)\bar{I} \tag{A15}$$

where

$$\bar{I}=\frac{I_1I_2}{I_1+I_2}$$

$$V_{1x}-d_{1R}\sin(\theta_1+\varphi_{1R})\Omega_1=\\ V_{3x}+d_{3R}\sin(\theta_3+\varphi_{3R})\Omega_3 \tag{A16}$$

$$V_{1y}+d_{1R}\cos(\theta_1+\varphi_{1R})\Omega_1=\\ V_{3y}-d_{3R}\cos(\theta_3+\varphi_{3R})\Omega_3 \tag{A17}$$

$$V_{2x}+d_{2Q}\sin(\theta_2+\varphi_{2Q})\Omega_2=\\ V_{4x}-d_{4Q}\sin(\theta_4+\varphi_{4Q})\Omega_4 \tag{A18}$$

$$V_{1x}-d_{1R}\sin(\theta_1+\varphi_{1R})\Omega_1=\\ V_{3x}+d_{3R}\sin(\theta_3+\varphi_{3R})\Omega_3 \tag{A19}$$

$$[V_{3x}+d_{3C}\sin(\theta_3+\varphi_{3C})\Omega_3]\cos\alpha_3+\\ [V_{3y}-d_{3C}\cos(\theta_3+\varphi_{3C})\Omega_3]\sin\alpha_3=0 \tag{A20}$$

$$[V_{4x}-d_{4C}\sin(\theta_4+\varphi_{4C})\Omega_4]\cos\alpha_4+\\ [V_{4y}+d_{4C}\cos(\theta_4+\varphi_{4C})\Omega_4]\sin\alpha_4=0 \tag{A21}$$

TABLES

Table 1 Data from the collision analysis in Example 1

Collision Geometry for Figure 1-a

	Vehicle 1	Vehicle 2
Mass (weight)	1800 kg (3969 lb)	27,000 kg (59,530 lb)
Initial Speed	15.0 m/s (33.6 mph)	-15.0 m/s (-33.6 mph)
Final Speed	-13.1 m/s (-29.4 mph)	-13.1 m/s (-29.4 mph)
Intervehicular Impulse	-50.7 kN-s (-11,400 lb-s)	50.7 kN-s (11,400 lb-s)

Collision Geometry for Figure 1-a

	Vehicle 3	Vehicle 4
Mass (weight)	1800 kg (3969 lb)	2400 kg (5292 lb)
Initial Speed	15.0 m/s (33.6 mph)	-15.0 m/s (-33.6 mph)
Final Speed	-2.14 m/s (-4.8 mph)	-2.14 m/s (-4.8 mph)
Intervehicular Impulse	-30.9 kN-s (-6950 lb-s)	30.9 kN-s (6950 lb-s)

Table 2 Vehicle input physical parameters for model validation

	Vehicle A - Body 1	Vehicle A - Body 3	Vehicle B - Body 2
Weight	13.7 kN (3087.5 lb)	9.8 kN (2196.6 lb)	10.4 kN (2337.7 lb)
Yaw moment of inertia	2152.0 kg-m^2 (1587.2 ft-lb-s^2)	2727.0 kg-m^2 (2011.3 t-lb-s^2)	1510.0 kg-m^2 (1113.7 t-lb-s^2)
Wheelbase	2.7 m (8.7 ft)	3.5 m (11.5 ft) [Hitch to axle]	2.6 m (8.4 ft)
Initial Speed	22.0 kph (13.7 mph)	22.0 kph (13.7 mph)	45.0 kph (28.0 mph)

Table 3 Comparison of the test results with analytical results

Alfa Romeo 164	Test Results	Analysis with $e = 0.2$ and $\mu = \mu_0$
ΔV_x of CG	-6.5 kph (-4.0 mph)	-4.4 kph (-2.7 mph)
ΔV_y of CG	21.5 kph (13.4 mph)	22.8 kph (14.2 mph)
$\lvert\Delta V\rvert$ of CG	22.5 kph (14.0 mph)	23.2 kph (14.4 mph)
PDOF	Not available	74.5°
Opel Ascona C		
ΔV_x of CG	7.5 kph (4.7 mph)	9.7 kph (6.0 mph)
ΔV_y of CG	-33.5 kph (-20.8 mph)	-32.7 kph (-20.3 mph)
$\lvert\Delta V\rvert$ of CG	34.3 kph (21.3 mph)	34.1 kph (21.2 mph)
PDOF	Not available	-16.5°
System		
Preimpact Energy	133.3 kJ (98.3×10^3 ft-lb)	133.3 kJ (98.3×10^3 ft-lb)
Postimpact Energy	71.5 kJ (52.7×10^3 ft-lb)	75.7 kJ (55.8×10^3 ft-lb)
Energy Loss	46.4%	43.2%

TABLES (cont.)

Table 4 Vehicle input and output parameters for Example 2

	Vehicle A - Body 1 Tractor	Vehicle A - Body 3 Semitrailer	Vehicle B - Body 2 Pickup Truck
Mass	6800.8 kg (466 lb-s^2/ft)	11,324.9 kg (776 lb-s^2/ft)	2262.1 kg (155 lb-s^2/ft)
Yaw Inertia	6779.1 N-m-s^2 (5000 ft-lb-s^2)	20,337.3 N-m-s^2 (15,000 ft-lb-s^2)	4880.9 N-m-s^2 (3600 ft-lb-s^2)
Initial Velocity (cg)	0.0 kph	0.0 kph	80.5 kph (50 mph)
Final Velocity (cg)	4.6 m/s (10.3 mph)	0.14 m/s (0.31 mph)	11.2 m/s (25.1 mph)
Magnitude of the impulse to meet the velocity constraint	N/A	5874.0 N-s (1320.5 lb-s)	N/A

FIGURES

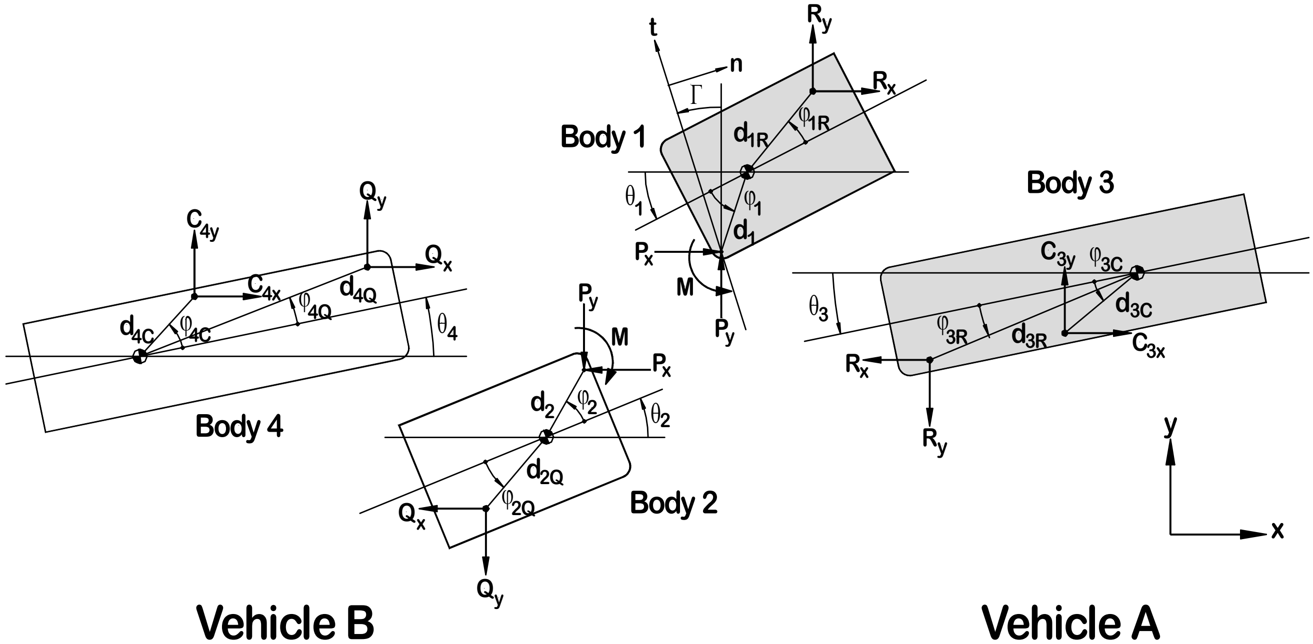

Figure 2 Free Body Diagrams for the four masses in a collision between two articulated vehicles

FIGURES (cont.)

Analysis of the Impact of Articulated Vehicles

5/5/06 6.3

INPUT:

Vehicle A {	Body 1:	Alfa Romeo	m_1:	1400.00	kg	I_1:	2,152.0	N-m-s^2	θ_1:	181.00	deg	v_{1x}:	6.25	m/s	v_{3x}:	6.25	m/s
	Body 3:	Hobby	m_3:	996.00	kg	I_3:	2,727.0	N-m-s^2	θ_3:	181.00	deg	v_{1y}:	0.11	m/s	v_{3y}:	0.11	m/s
Vehicle B {	Body 2:	Opel Ascona C	m_2:	1060.00	kg	I_2:	1,510.0	N-m-s^2	θ_2:	90.00	deg	v_{2x}:	0.00	m/s	v_{4x}:	0.00	m/s
	Body 4:	Semitrailer 2	m_4:	0.00	kg	I_4:	0.0	N-m-s^2	θ_4:	0.00	deg	v_{2y}:	12.78	m/s	v_{4y}:	0.00	m/s

9.80665	RUN impactAV	d_1:	0.89	m	d_{1R}:	2.51	m	ϕ_1:	-73.29	deg	ϕ_{1R}:	0.00	deg	ω_1:	0.0 °/s
1.466666667		d_{3C}:	0.00	m	d_{3R}:	3.25	m	ϕ_{3C}:	0.00	deg	ϕ_{3R}:	0.00	deg	ω_3:	0.0 °/s
	Unit Conversion	d_2:	1.84	m	d_{2Q}:	0.00	m	ϕ_2:	8.29	deg	ϕ_{2Q}:	0.00	deg	ω_2:	0.0 °/s
SI		d_{4C}:	0.00	m	d_{4Q}:	0.00	m	ϕ_{4C}:	0.00	deg	ϕ_{4Q}:	0.00	deg	ω_4:	0.0 °/s

If there is a known velocity constraint for rigid body 3 and/or 4, enter the angles (α_3, α_4). Otherwise, enter "none" (lowercase w/o "").

α_3:	none	deg
α_4:	none	deg

If known, enter the external pin impulse for Vehicles A and B (R and Q, respectively). Otherwise type "unknown" (lowercase w/o "").

R_x:	unknown	N-s	Γ	90.00	deg
R_y:	unknown	N-s	e	0.20	
Q_x:	unknown	N-s	μ	100.00	% μ_0
Q_y:	unknown	N-s	e'	-1	e' = -1 means that the moment impulse is zero

OUTPUT:

Initial Velocities:	v_{1x}:	6.25	m/s	v_{1y}:	0.11	m/s	ω_1:	0.00	°/s	v_1:	6.25	m/s	22.50	km/hr
	v_{3x}:	6.25	m/s	v_{3y}:	0.11	m/s	ω_3:	0.00	°/s	v_3:	6.25	m/s	22.50	km/hr
	v_{2x}:	0.00	m/s	v_{2y}:	12.78	m/s	ω_2:	0.00	°/s	v_2:	12.78	m/s	46.00	km/hr
	v_{4x}:	0.00	m/s	v_{4y}:	0.00	m/s	ω_4:	0.00	°/s	v_4:	0.00	m/s	0.00	km/hr
Final Velocities:	V_{1x}:	5.02	m/s	V_{1y}:	6.43	m/s	Ω_1:	57.43	°/s	V_1:	8.16	m/s	29.37	km/hr
	V_{3x}:	5.12	m/s	V_{3y}:	0.88	m/s	Ω_3:	53.58	°/s	V_3:	5.19	m/s	18.69	km/hr
	V_{2x}:	2.69	m/s	V_{2y}:	3.71	m/s	Ω_2:	-100.09	°/s	V_2:	4.58	m/s	16.48	km/hr
	V_{4x}:	0.00	m/s	V_{4y}:	0.00	m/s	Ω_4:	0.00	°/s	V_4:	0.00	m/s	0.00	km/hr
Impulse Values:	R_x:	1,128.2	N-s	R_y:	-765.1	N-s	R:	1,363.2	N-s	ΔV_1:	6.44	m/s	23.19	km/hr
	P_x:	-2,849.9	N-s	P_y:	9,616.6	N-s	P:	10,030.0	N-s	ΔV_2:	9.46	m/s	34.06	km/hr
	P_N:	9,616.6	N-s	P_T:	2,849.9	N-s	M:	0.0	N-m-s	ΔV_3:	1.37	m/s	4.93	km/hr
	Q_x:	0.0	N-s	Q_y:	0.0	N-s	Q:	0.0	N-s	ΔV_4:	0.00	m/s	0.00	km/hr

Energy Values:

Initial energy of Veh A	T_{IA}:	46,796.9 N-m	μ :	0.296	No Sliding at Separation
Final energy of Veh A	T_{FA}:	62,283.6 N-m	μ_0:	0.296	
Initial energy of Veh B	T_{IB}:	86,537.0 N-m	e:	0.20	
Final energy of Veh B	T_{FB}:	13,412.9 N-m	e':	-1.00	

Initial System Kinetic Energy:	133,333.8 N-m
Final System Kinetic Energy:	75,696.5 N-m
System Energy Loss:	57,637.3 N-m
Percent System Energy Loss:	43.2 %

Figure 7 Spreadsheet results for model validation with $e = 0.2$ and $\mu = \mu_0$